


Article

Fluorometric Detection of Thiamine Based on Hemoglobin–Cu₃(PO₄)₂ Nanoflowers (NFs) with Peroxidase Mimetic Activity

Hangjin Zou, Yang Zhang, Chuhan Zhang, Rongtian Sheng, Xinming Zhang and Yanfei Qi * 

School of Public Health, Jilin University, Changchun 130021, Jilin, China; zouhj18@mails.jlu.edu.cn (H.Z.); yangzhang19@mails.jlu.edu.cn (Y.Z.); zhangch18@mails.jlu.edu.cn (C.Z.); shengrt19@mails.jlu.edu.cn (R.S.); xmzhang19@mails.jlu.edu.cn (X.Z.)

* Correspondence: qianfei@jlu.edu.cn

Received: 30 September 2020; Accepted: 4 November 2020; Published: 7 November 2020



Abstract: Component analysis plays an important role in food production, pharmaceuticals and agriculture. Nanozymes have attracted wide attention in analytical applications for their enzyme-like properties. In this work, a fluorometric method is described for the determination of thiamine (TH) (vitamin B₁) based on hemoglobin–Cu₃(PO₄)₂ nanoflowers (Hb–Cu₃(PO₄)₂ NFs) with peroxidase-like properties. The Hb–Cu₃(PO₄)₂ NFs catalyzed the decomposition of H₂O₂ into ·OH radicals in an alkaline solution that could efficiently react with nonfluorescent thiamine to fluoresce thiochrome. The fluorescence of thiochrome was further enhanced with a nonionic surfactant, Tween 80. Under optimal reaction conditions, the linear range for thiamine was from 5 × 10^{−8} to 5 × 10^{−5} mol/L. The correlation coefficient for the calibration curve and the limit of detection (LOD) were 0.9972 and 4.8 × 10^{−8} mol/L, respectively. The other vitamins did not bring about any obvious changes in fluorescence. The developed method based on hybrid nanoflowers is specific, pragmatically simple and sensitive, and has potential for application in thiamine detection.

Keywords: food analysis; fluorometric method; thiamine; nanozymes; protein-inorganic nanoflowers

1. Introduction

Thiamine (TH) (vitamin B₁) is an important water-soluble vitamin in the human body [1,2]. It is involved in various metabolic processes [3], and the phosphorylated derivative thiamine diphosphate is a transketolase for the substances necessary for the activity of mitochondrial pyruvate [4]. Humans and other mammals cannot synthesize thiamine by themselves, and instead, take in vitamin B₁ from the outside world [5]. The recommended daily intake of vitamin B₁ in adults is 0.5–1 mg [6]. A severe deficiency of vitamin B₁ can cause athlete's foot, neuralgia, optic neuropathy, anorexia and KORSAKOFF syndrome [7–9]. Between 3 and 5 mg/kg of vitamin B₁ are required as a food additive in rice, wheat and miscellaneous grains. The related detection methods for vitamin B₁ involve spectrophotometry [10,11], chemiluminescence [12], chromatography [13–15], fluorescence [7,16,17], electrochemistry [18] and capillary electrophoresis [19]. Notably, although some of them are capable of accurate or high-throughput monitoring of amounts of vitamin B₁ and have even been practically used in food quality control, these methods are restricted to expensive, low selectivity or complicated experimental conditions. Among these methods, the fluorometric method based on the oxidation of thiamine to thiochrome by potassium hexacyanoferrate (III) in alkaline solution is the most widely used. However, the thiochrome yield (about 67%) of the reaction using hexacyanoferrate as an oxidant is not high. Therefore, this method is often improved by substituting hexacyanoferrate with other materials, such as graphene quantum dot-capped gold nanoparticles [20] and oxygen

vacancy-engineered PEGylated MoO_{3-x} nanoparticles [21]. These materials offer improved sensitivity and assay simplicity with unexpected properties including large surface-to-volume ratio, high stability and enhanced oxidizing capability.

Since Zare et al. [22] first reported protein-inorganic nanoflowers, a variety of new protein-inorganic hybrid nanoflowers have been synthesized with greater specific surface area, better stability and cooperatively enhanced catalysis features. The composite materials have shown potential for application in sensors and analytical devices and in biocatalysis. Qu et al. further explored the peroxidase-like activity of protein-inorganic hybrid nanoflowers and performed self-activated cascade reactions [23]. Recently, Pang et al. reported Hb- $\text{Cu}_3(\text{PO}_4)_2$ nanoflowers (NFs) with hemoglobin and $\text{Cu}_3(\text{PO}_4)_2$ and enhanced peroxidase catalytic activity in the detection of hydrogen peroxide in an acetic acid buffer solution [24]. Yang et al. synthesized horseradish peroxidase- $\text{Cu}_3(\text{PO}_4)_2 \cdot 3\text{H}_2\text{O}$ hybrid nanoflowers for the fast and sensitive visual detection of H_2O_2 and phenol [25]. Despite this attractive feature of enzyme- $\text{Cu}_3(\text{PO}_4)_2 \cdot 3\text{H}_2\text{O}$ hybrid nanoflowers, the advantages and properties of hybrid nanoflowers have not yet been fully demonstrated. In this paper, we first investigate the enzyme-mimic activity of Hb- $\text{Cu}_3(\text{PO}_4)_2$ NFs in an alkaline solution in detail. A Hb- $\text{Cu}_3(\text{PO}_4)_2$ NF-based fluorometric method is developed for the detection of thiamine. Through a fluorometric assay, the alkaline solution, substrate, Hb- $\text{Cu}_3(\text{PO}_4)_2$ NF concentrations and Tween 80 are investigated. Under optimal reaction conditions, the resulting sensor displayed a rapid response and high sensitivity to thiamine.

2. Materials and Methods

2.1. Materials and Chemicals

All the chemicals used were of analysis grade without further purification. Hemoglobin (Hb, from bovine blood) was purchased from Sigma-Aldrich. Thiamine, L-ascorbic acid (Vc) and folic acid (VB_9) were obtained from Guoyao Chemical Research Institute (Shenyang, China). NaCl, KCl, NaHCO_3 , NaHPO_4 , NaH_2PO_4 , NaHSO_4 , NaOH, glucose and hydrogen peroxide (H_2O_2 , 30%) were purchased from Beijing Chemical Works (Beijing, China). 1,2-diaminobenzene (OPD) and CuSO_4 were purchased from Tianjin Guangfu Fine Chemical Research Institute (Tianjin, China). The water used in the experiments was purified. The ρ of the water was $18 \text{ M}\Omega \cdot \text{cm}$.

2.2. Instrument

The fluorescence measurements were performed on a Shimadzu RF-5301 PC fluorophotometer (Kyoto, Japan) and Microplate reader (BioTek, Winooski, VT, USA). A 1 cm path length quartz cuvette and 96-well microplates were used in the experiments. The widths of the excitation and emission slits of the fluorophotometer were set to 3.0 and 3.0 nm, respectively. The Fourier-transform infrared (FTIR) spectrum was recorded in the range of $400\text{--}4000 \text{ cm}^{-1}$ on KBr (FTIR IRAffinity-1s, Shimadzu, Japan). The pH measurements were performed by a PHS-25 pH meter (Shanghai INESA Scientific Instrument Co. Ltd., Shanghai, China). The UV-vis spectrum was recorded in the range of $200\text{--}1100 \text{ nm}$ on a UV-vis spectrophotometer (Puxi Inc., Beijing, China). Zeta potential was measured by photon correlation spectroscopy using a Zetasizer (Nano-ZS90). A scanning electron microscopy (SEM) image was characterized by a Zeiss Merlin at 1.0 kV. The purified water was obtained from a SMART-N Heal Force Water Purification System (Shanghai Canrex Analytic Instrument Co., Ltd., Pudong, Shanghai, China). The nanoparticle surface charge was determined with a Malvern Zetasizer. The P element was determined by an inductively coupled plasma mass spectrometer (ELAN DRC-e, PerkinElmer, Concord, Ontario, Canada).

2.3. Synthesis of Hb- $\text{Cu}_3(\text{PO}_4)_2$ NFs

Hb- $\text{Cu}_3(\text{PO}_4)_2$ NFs were prepared according to a method described in the literature, with some modifications [24]. Briefly, 2 mL of CuSO_4 aqueous solution (120 mM) was added into 300 mL of phosphate-buffered saline (PBS) solution (0.1 M, pH 7.4) containing 30 mg Hb. After incubation at 25°C

for 72 h, the turquoise precipitates of Hb-Cu₃(PO₄)₂ NFs were collected by centrifugation (3000 rpm for 5 min) and washed with ultrapure water three times.

2.4. Detection of Reactive Hydroxyl Radical (\cdot OH) Production

The hydroxyl radical (\cdot OH) production was measured using a fluorescence method. Terephthalic acid (TA) was used as a fluorescence probe for detection of \cdot OH in H₂O₂. First, 75 μ L of 25 mM TA in the NaOH (pH 13) solution was added into the 3 mL of PBS (pH 7.4) containing 100 mM H₂O₂ and 2 mg/mL Hb-Cu₃(PO₄)₂ NFs. After 1 h incubation in the dark, the solution was examined for fluorometric measurements. Fluorescence spectra were obtained with an excitation wavelength of 315 nm and the emission spectra were recorded at a wavelength of 425 nm.

2.5. Enzyme-like Activity and Kinetic Parameter of Hb-Cu₃(PO₄)₂ NFs

The enzyme-like activity of freshly synthesized Hb-Cu₃(PO₄)₂ NFs was investigated spectrophotometrically by measuring the formation of DAP (2,3-diaminophenazine) from OPD at 450 nm ($\epsilon = 21,000 \text{ M}^{-1} \times \text{cm}^{-1}$) using a multiwell plate reader. Typically, 10 μ L OPD (2 mM) was added into different 170 μ L buffer solutions, followed by 10 μ L Hb-Cu₃(PO₄)₂ NFs (2 mg/mL) and 10 μ L H₂O₂ (100 mM) at 37 °C. The activity of the Hb-Cu₃(PO₄)₂ NFs at different pH values (pH 3–13) was studied using similar conditions as those described above. The pH of the different solutions was measured using a pH meter. Additionally, the buffers with pH values from 9 to 13 were prepared from the mixture of 0.2 M disodium hydrogen phosphate and a sufficient quantity of 1 M sodium hydroxide. pH values from 5 to 8 were obtained from the mixture of 0.2 M disodium hydrogen phosphate and 0.2 M sodium dihydrogen phosphate. Solutions with pH values of 3 and 4 were obtained from the mixture of 0.1 M citric acid and sodium citrate.

The steady-state kinetics of Hb-Cu₃(PO₄)₂ NFs were performed by varying the concentrations of H₂O₂ (0–0.1 M) or OPD (0–2 mM) one at a time. The reaction was carried out in 160 μ L phosphate buffers (pH 10) and monitored spectrophotometrically every 300 s using a multiwell plate reader. The kinetic curves were adjusted to the Michaelis–Menten model using the Origin (version 8.0, OriginLAB Corporation, Boston, MA, USA) software. The apparent kinetic parameters, Michaelis–Menten constant (K_m) and maximum rate of reaction (V_{max}) were calculated.

2.6. Condition Optimization

The reaction parameters of the time, pH, H₂O₂ and Hb-Cu₃(PO₄)₂ NF concentrations as well as the fluorescence sensitizer (Tween 80) were investigated. Typically, 160 μ L of different buffers (pH 8–13), 10 μ L of different concentrations of Hb-Cu₃(PO₄)₂ NFs (0–4 mg/mL), 10 μ L of different concentrations of H₂O₂ (0–10 M) and 20 μ L of 1 mM thiamine were mixed at room temperature. The fluorescence intensities were recorded every 15 min.

2.7. Fluorescent Detection of Thiamine

The quantitative determination of thiamine using a Hb-Cu₃(PO₄)₂ NF-catalyzed fluorescent assay in the presence of H₂O₂ was performed as follows. A 160 μ L Na₂HPO₄-NaOH buffer (pH 10) with 0.4% Tween 80, 10 μ L of 100 mM H₂O₂, 20 μ L of different concentrations of thiamine (0.0001–10 mM) and 10 μ L of 2 mg/mL Hb-Cu₃(PO₄)₂ NFs were mixed at room temperature, sequentially. Then, the mixtures were placed in a constant temperature incubator at 37 °C for 5 min. The fluorescence values of the above-mentioned solutions were measured using a microplate reader with an excitation wavelength of 370 nm. The emission spectra of these reaction solutions were recorded at a wavelength of 441 nm.

3. Results and Discussion

3.1. Characterization of Hb-Cu₃(PO₄)₂ NFs

The Hb-Cu₃(PO₄)₂ NFs were characterized using IR, UV-vis, SEM and Zetasizer methods. The IR spectra of CuSO₄, hemoglobin and Hb-Cu₃(PO₄)₂ NFs are shown in Figure 1a. The main characteristic vibration peaks of Hb were found at 1134, 1317 and 1679 cm⁻¹ and attributed to ν(C-N) and ν(N-H), respectively. The peak found at 3306 cm⁻¹ was assigned to the O-H of water. The spectrum of Hb-Cu₃(PO₄)₂ NFs maintained the characteristic peaks of Hb at 1049, 1652 and 1734 cm⁻¹ assigned to ν_{as}(N-H) and ν_{as}(C-N). The bands at 1041 and 1162 cm⁻¹ were attributed to P-O and P=O vibrations. The existence of a phosphate element was also proved using an inductively coupled plasma mass spectrometer. The result was similar to that found in the literature [24]. As shown in Figure 1b, the UV-vis spectrum of Hb exhibited an absorbance at 254 nm. Cu²⁺ exhibited an absorbance at 800 nm. The characteristic peaks of Cu²⁺ and Hb were observed in the spectrum of the Hb-Cu₃(PO₄)₂ NFs. The morphological structure of Hb-Cu₃(PO₄)₂ NFs obtained by SEM is shown in Figure 1c. The SEM images indicate that Hb-Cu₃(PO₄)₂ NFs have a flower-like structure with a size of about 15 μm. The surface zeta potential measurements show that the ζ of CuSO₄, hemoglobin and Hb-Cu₃(PO₄)₂ NFs were approximately -2.1 mV, 10.7 mV and -4.5 mV, respectively, as shown in Figure 1d. The ζ and the SEM consistently proved that the Hb-Cu₃(PO₄)₂ NFs were successfully synthesized.

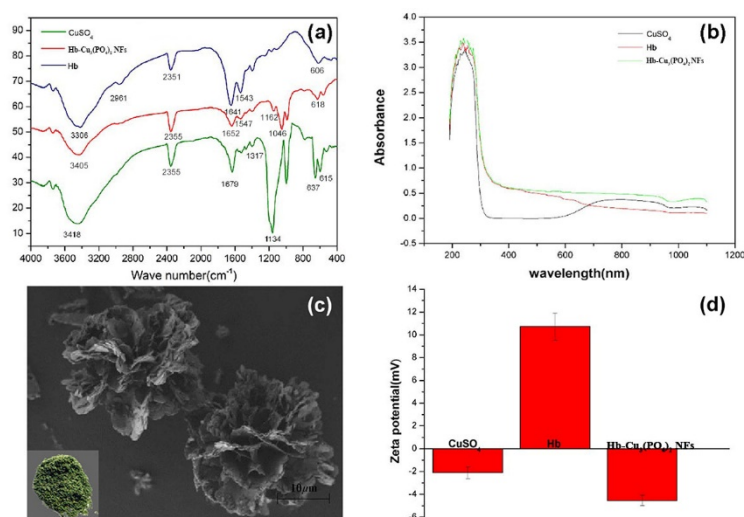


Figure 1. (a) IR spectra of CuSO₄ (green line), Hb (blue line) and Hb-Cu₃(PO₄)₂ NFs (red line); (b) UV-vis absorptions of CuSO₄ (blue line), Hb (red line) and Hb-Cu₃(PO₄)₂ NFs (green line); (c) SEM image of Hb-Cu₃(PO₄)₂ NFs; (d) Zeta potentials of CuSO₄, Hb and Hb-Cu₃(PO₄)₂ NFs.

3.2. Enzyme-Like Activities and Kinetic Parameters of Hb-Cu₃(PO₄)₂ NFs

In order to clarify the mechanism of Hb-Cu₃(PO₄)₂ NFs, terephthalic acid (TA) was used as a fluorescence probe for the tracking of ·OH because it can capture ·OH and generate a fluorescent product, 2-hydroxyterephthalic acid (HTA), at 425 nm. As shown in Figure S1, the control groups, TA, TA with H₂O₂ and TA with Hb-Cu₃(PO₄)₂ NFs, did not show significant intensity for HTA. Only in the presence of Hb-Cu₃(PO₄)₂ NFs and H₂O₂ could fluorescence be found. This result supports the hypothesis that Hb-Cu₃(PO₄)₂ NFs can catalyze H₂O₂ to generate ·OH, thus demonstrating the peroxidase-like activities of Hb-Cu₃(PO₄)₂ NFs. Therefore, eight systems were established to prove that Hb-Cu₃(PO₄)₂ NFs are peroxidases. Figure 2 clearly shows that fluorescence intensity increased with the presence of Hb-Cu₃(PO₄)₂ NFs and H₂O₂. No fluorescence intensity was observed in the absence of H₂O₂ or Hb-Cu₃(PO₄)₂ NFs. In addition, an equal amount of Hb or copper ion (1 mg/mL) in the presence of both TH and H₂O₂ showed weak fluorescence (Figure S2). These results indicate

that Hb-Cu₃(PO₄)₂ NFs can catalytically activate H₂O₂ decomposition to generate ·OH radicals and lead to more efficient oxidation of thiamine.

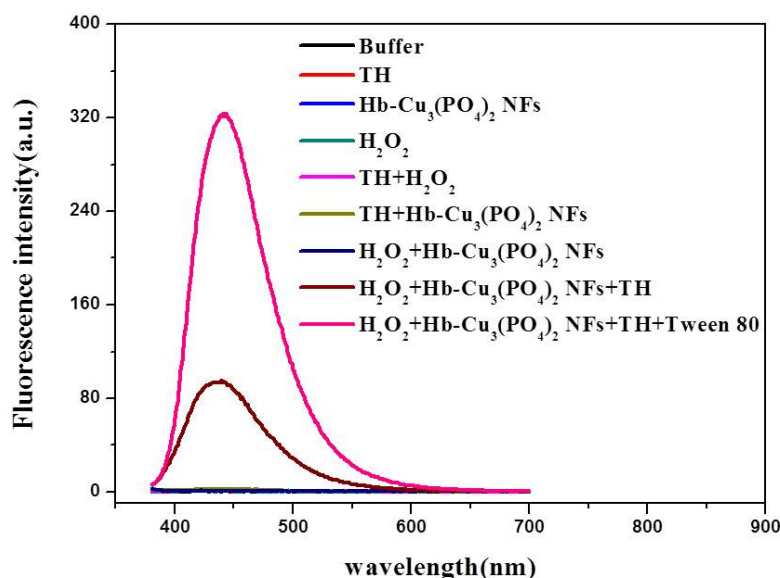


Figure 2. Fluorescence spectra of Na₂HPO₄-NaOH (pH 10) (black line), TH (red line), Hb-Cu₃(PO₄)₂ NFs (light blue line), H₂O₂ (dark green line), TH + H₂O₂ (purple line), TH + Hb-Cu₃(PO₄)₂ NFs (light green line), Hb-Cu₃(PO₄)₂ NFs + H₂O₂ (dark blue line), TH + H₂O₂ + Hb-Cu₃(PO₄)₂ NFs (brown line), TH + H₂O₂ + Hb-Cu₃(PO₄)₂ NFs + Tween 80 (pink line).

According to a previous report [24], Hb-Cu₃(PO₄)₂ NFs showed peroxidase activity under acidic pH conditions. However, the above fluorescence experiment results indicate that Hb-Cu₃(PO₄)₂ NFs were highly active even at pH 10. Therefore, the effect of pH on the enzyme activity of Hb-Cu₃(PO₄)₂ NFs was throughout measured by varying the pH and keeping the OPD and/or H₂O₂ concentration constant. As shown in Figure S3, the peroxidase-like activity of Hb-Cu₃(PO₄)₂ NFs was present at pH 3 to 11. Interestingly, as shown in Figure S4, it was found that Hb-Cu₃(PO₄)₂ NFs could catalyze oxidase reactions with OPD in the absence of H₂O₂ and showed oxidase-like activity at pH 12 and 13. In contrast, no obvious absorbance was found for other pH solutions. The results indicate that the Hb-Cu₃(PO₄)₂ NFs actualized dual enzyme-like activity. In Figure S5, it can be observed that the OPD oxidation rate catalyzed by the Hb-Cu₃(PO₄)₂ NFs was dependent on the concentration of nanoflowers and period of time at pH 10. The absorbance values were increased with an increasing amount of NFs and length of time. According to a method described previously [26–30], the mechanism of peroxidase-like catalytic activities of Hb-Cu₃(PO₄)₂ NFs can be further investigated using steady-state kinetic assays at pH 10. As shown in Figure S6, a typical Michaelis–Menten curve was obtained for Hb-Cu₃(PO₄)₂ NFs in the presence of H₂O₂ and OPD, respectively. The Michaelis–Menten constant (K_m) and the maximum initial velocity (V_{max}) were acquired from the Michaelis–Menten curve. The K_m of Hb-Cu₃(PO₄)₂ NFs with OPD and H₂O₂ as substrates was 0.02 mM and 1.8 mM, respectively. The V_{max} of Hb-Cu₃(PO₄)₂ NFs with OPD and H₂O₂ as substrates was $1.96 \times 10^{-8} \text{ M} \times \text{S}^{-1}$ and $1.38 \times 10^{-8} \text{ M} \times \text{S}^{-1}$, respectively. Overall, the enhancement in the enzymatic activity of Hb-Cu₃(PO₄)₂ NFs can be ascribed to the possible stabilization of the NF-like structure of Hb through high surface area and confinement, resulting in higher accessibility of the substrate to the active sites. Thus, thiamine could be oxidized to yield fluorescent thiochrome in a basic solution. As shown in Figure 3, the fluorescence values of thiochrome were measured by a fluorescence spectrophotometer with a maximum emission of 441 nm and an excitation wavelength of 370 nm.

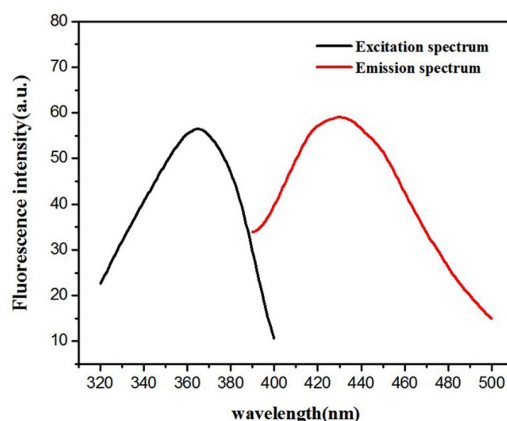


Figure 3. The excitation and emission spectra for thiochrome.

3.3. Condition Optimization

A series of experiments were conducted to establish the optimum analytical conditions for the oxidation of thiamine by H_2O_2 with $\text{Hb-Cu}_3(\text{PO}_4)_2$ NFs as catalyst. The parameters investigated were reaction time; the concentrations of pH, H_2O_2 and $\text{Hb-Cu}_3(\text{PO}_4)_2$ NFs; and the fluorescence sensitizer, Tween 80.

3.3.1. Effect of pH and Reaction Time

The solution pH was an important factor which influenced the peroxidase-like activity of the $\text{Hb-Cu}_3(\text{PO}_4)_2$ NFs. As shown in Figure 4a, when using different phosphate buffers ranging from pH 8 to 13, the peak of the maximum fluorescence intensity was obtained with a phosphate buffer of pH 10. The fluorescence intensity of thiochrome rapidly increased with reaction time, initially from 0 to 300 s, and then the values slowly reached a plateau, indicating that the H_2O_2 was completely consumed by oxidation of the substrate TH. Thus, 300 s was chosen as the optimal reaction time for a phosphate buffer of pH 10.

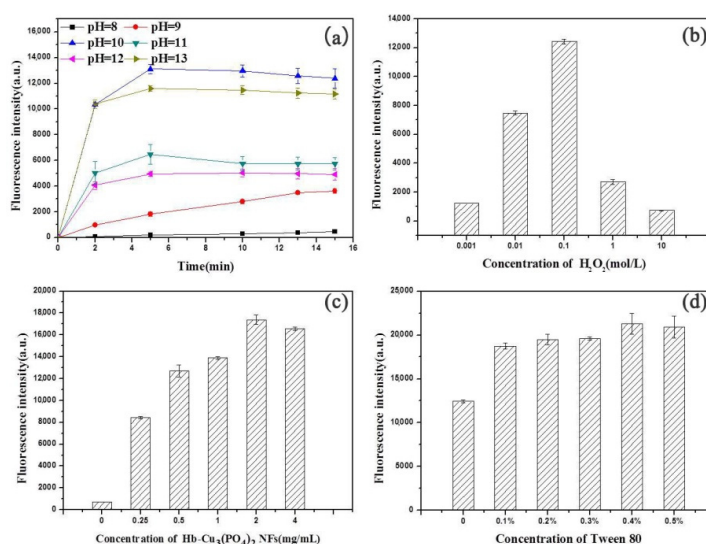


Figure 4. The optimization of experimental conditions: (a) reaction time and pH, (b) H_2O_2 concentration, (c) $\text{Hb-Cu}_3(\text{PO}_4)_2$ NF concentration and (d) the amount of Tween 80. Conditions: (a) H_2O_2 , 1×10^{-3} mol/L; $\text{Hb-Cu}_3(\text{PO}_4)_2$ NFs, 2 mg/mL; thiamine, 1×10^{-3} mol/L. (b) $\text{Hb-Cu}_3(\text{PO}_4)_2$ NFs, 2 mg/mL; thiamine, 1×10^{-3} mol/L; pH, 10; incubation time, 5 min. (c) H_2O_2 , 1×10^{-3} mol/L; thiamine, 1×10^{-3} mol/L; pH, 10; incubation time, 5 min. (d) H_2O_2 , 1×10^{-3} mol/L; $\text{Hb-Cu}_3(\text{PO}_4)_2$ NFs, 2 mg/mL; thiamine, 1×10^{-3} mol/L; pH, 10; incubation time, 5 min.

3.3.2. Effect of H₂O₂ Concentration

To achieve a maximum oxidation rate of the thiamine, optimization of hydrogen peroxide concentration was necessary. As shown in Figure 4b, the fluorescence intensity increased quickly with the concentration of H₂O₂ up to 100 mM and then decreased. Therefore, 100 mM H₂O₂ was selected as the optimum concentration.

3.3.3. Effect of Hb–Cu₃(PO₄)₂ NF Concentration

In order to achieve the optimal oxidation rate of the thiamine catalyzed by Hb–Cu₃(PO₄)₂ NFs, the effect of Hb–Cu₃(PO₄)₂ NF concentrations (0–4 mg/mL) on the fluorescence of thiochrome was investigated. As shown in Figure 4c, the fluorescence intensity first increased and then slowly decreased with an increase in Hb–Cu₃(PO₄)₂ NF concentration. The maximum fluorescence intensity in the system was obtained at 2 mg/mL of Hb–Cu₃(PO₄)₂ NF solution. Thus, 2 mg/mL was selected for the Hb–Cu₃(PO₄)₂ NFs as the optimal concentration.

3.3.4. Effect of Tween 80 Concentration

Tween 80, a hydrophilic nonionic surfactant, had been utilized in the drug loading and the biosensor fields for its hydrophilicity and low toxicity [31–33]. Previous reports have shown that Tween 80 can enhance the fluorescence of a system. For example, it has been used in fluorescence detections of nicotinamide [34] and nifanib [35]. In this work, Tween 80 was added in the fluorescence determination for thiamine. The effect of the amount of Tween 80 (0.1–0.5%) was investigated with the other parameters kept constant. As shown in Figure 4d, the fluorescence intensity first increased and then slowly decreased along with an increase in the amount of Tween 80. The maximum fluorescence intensity in the system was obtained at a Tween 80 solution of 0.4%. Therefore, a Tween 80 solution of 0.4% was chosen as the optimal concentration.

3.4. Calibration Curve for Thiamine Detection

Under the optimized reaction conditions, the relationship between the fluorescence intensity and thiamine concentration catalyzed by Hb–Cu₃(PO₄)₂ NFs was investigated. As shown in Figure 5, the fluorescence intensity increased with increasing concentration of thiamine. The linear regression equation was $F = 19.247 + 2.452 \times 10^8 \times C_{\text{thiamine}}$ with a correlation coefficient of 0.9984. There was a good linear correlation between the fluorescence intensity and the thiamine concentration in the range of 5×10^{-8} to 5×10^{-5} M. The lower limit of detection of Hb–Cu₃(PO₄)₂ NFs for thiamine was found to be 4.8×10^{-8} M, which is similar to the HRP-based fluorescent method for the detection of thiamine [36]. It is almost believable that its ability to detect thiamine is similar to the HRP-based fluorescent method. Compared with HRP, nanozymes have the advantages of being highly stable against denaturing, low-cost, easy to store and suitable for treatment. The mimic enzyme activity of Hb–Cu₃(PO₄)₂ NFs was firstly utilized in fluorometric sensing of thiamine under basic conditions. Compared with other systems for the determination of thiamine, as shown in Table 1, the proposed method based on Hb–Cu₃(PO₄)₂ NFs is on a par with other fluorescence methods. Additionally, the synthesis of the Hb–Cu₃(PO₄)₂ NFs was convenient and simple. Therefore, the method should be a potential candidate for fluorescence sensors of thiamine.

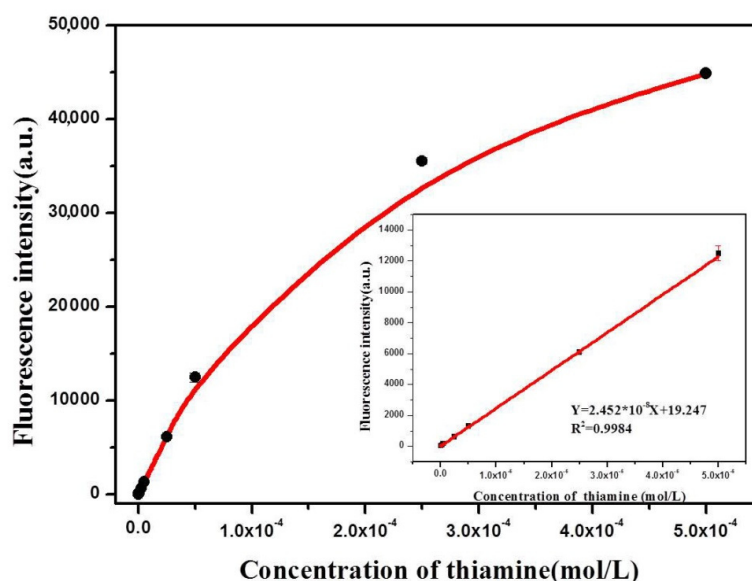


Figure 5. Fluorescence intensity change of the solutions containing Hb–Cu₃(PO₄)₂ NFs upon the addition of different concentrations of thiamine (5×10^{-9} to 5×10^{-4} mol/L). The inset shows the linear calibration plot for TH. Error bar: RSD ($n = 3$).

Table 1. Comparison of the detection of thiamine in different fluorescent systems.

System	Linear Range	Detection Limit	Reference
TBP/IMS/FRET	5–240 nM	2 nmol/g	[36]
e-PNPs/ESIPT	0.1–25 μ M	2.6 nM	[7]
O-phen/Zn ²⁺	0.84–80.0 μ M	0.25 μ M	[37]
HKUST-1	4–700 μ M	1 μ M	[38]
C-dots/Cu ²⁺	10–50 μ M	0.28 nM	[39]
HRP	0.08–49.90 μ M	0.04 μ M	[2]
Cu ²⁺	0.89–17.85 μ M	0.50 μ M	[40]
Hb–Cu ₃ (PO ₄) ₂ NFs	0.05–50 μ M	0.048 μ M	This work

TBP: thiamine periplasmic binding protein; IMS: immunomagnetic separation; FRET: fluorescence resonance energy transfer; e-PNPs: exhibiting polymer nanoparticles; ESIPT: excited-state intramolecular proton transfer; O-phen: o-phenanthroline; HKUST-1: peroxidase-like activity of copper-based MOFs; C-dots: carbon dots; HRP: horseradish peroxidase.

3.5. Determination of Thiamine in Functional Food Tablet Samples

In order to evaluate the feasibility of the proposed method based on Hb–Cu₃(PO₄)₂ NFs, the concentrations of thiamine in multivitamin functional food tablets samples were analyzed under the optimal conditions. As shown in Table 2, the recovery level of the developed approach was between 103.20 and 115.20%. The result suggests that the developed method is accurate and reliable for thiamine detection in real samples.

Table 2. The recovery of thiamine in tablets by standard addition.

Sample	Added (μ M)	Detected (μ M)	Recovery (%)
1	25	25.8 \pm 4.35	103.2
2	0.50	0.57 \pm 0.03	115.2
3	0.25	0.27 \pm 0.19	107.2

3.6. Interference Study

The selectivity of the proposed method was examined by comparing the fluorescence change of the solution with thiamine (0.3 mg/mL) with other coexistence substrates (30 mg/mL) including K⁺,

Na^+ , Cl^- , HCO_3^- , glucose, starch, VB_2 , VB_7 , VB_9 and Vc. These control compounds are usually found in foods. As shown in Figure 6, the fluorescence of the solution changed only when thiamine was added to the mixture. The addition of the other molecules, in contrast, had no obvious effect on the fluorescence of the solutions. Thus, the proposed fluorometric method displayed a high selectivity for the determination of thiamine.

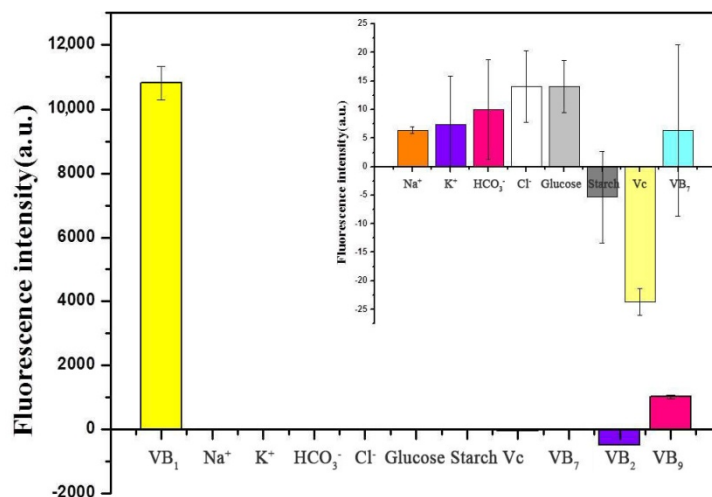


Figure 6. Interference study for the determination of thiamine. Concentrations of Na^+ , K^+ , HCO_3^- , Cl^- , glucose, starch, Vc, VB_7 , VB_2 and VB_9 : 30 $\mu\text{g}/\text{mL}$. Inset: the amplified fluorescence intensity of Na^+ , K^+ , HCO_3^- , Cl^- , glucose, starch, Vc and VB_7 .

4. Conclusions

In summary, a new fluorometric enhancement method for the detection of thiamine has been demonstrated. The peroxidase-like activity of $\text{Hb-Cu}_3(\text{PO}_4)_2$ NFs was first found in a basic solution. Under the optimal conditions, H_2O_2 could be decomposed into $\cdot\text{OH}$ radicals by $\text{Hb-Cu}_3(\text{PO}_4)_2$ NFs that oxidize thiamine rapidly and efficiently. A linear correlation was established between fluorescence intensity and the concentration of thiamine from 0.05–50 μM with a detection limit of 48 nM. Future research may focus on attempts to explore the new protein–inorganic hybrid nanoflowers or analytes in the detecting systems.

Supplementary Materials: The following are available online at <http://www.mdpi.com/1424-8220/20/21/6359/s1>. Figure S1: Fluorescence spectra for detection of hydroxyl radicals $\cdot\text{OH}$ with different controls; Figure S2: The fluorescence intensities of thiochrome in the catalytic activities of CuSO_4 , hemoglobin and $\text{Hb-Cu}_3(\text{PO}_4)_2$ NFs with the same concentration of 1 mg/mL; Figure S3: The pH Dependency with catalytic activity of $\text{Hb-Cu}_3(\text{PO}_4)_2$ NFs using pH 3–11; Figure S4: The pH Dependency with oxidase activity of $\text{Hb-Cu}_3(\text{PO}_4)_2$ NFs; Figure S5: Dependency of OPD oxidation activity on the $\text{Hb-Cu}_3(\text{PO}_4)_2$ NFs concentration (0.03125–1mg/mL) and time(5–15min); Figure S6: Steady-state kinetic study of $\text{Hb-Cu}_3(\text{PO}_4)_2$ NFs.

Author Contributions: Conceptualization, H.Z. and Y.Q.; methodology, H.Z. and Y.Q.; software, Y.Z.; validation, C.Z., Y.Z. and R.S.; writing—original draft preparation, H.Z. and Y.Z.; writing—review and editing, X.Z.; visualization; Y.Q.; funding acquisition, Y.Q. All authors have read and agreed to the published version of the manuscript.

Funding: This research was funded by NSFC (81402719, 82073602) and Norman Bethune Program of Jilin University (2015228).

Conflicts of Interest: The authors declare no conflict of interest.

References

1. Wang, Y. Simultaneous determination of uric acid, xanthine and hypoxanthine at poly(pyrocatechol violet)/functionalized multi-walled carbon nanotubes composite film modified electrode. *Colloid Surf. B* **2011**, *88*, 614–621. [[CrossRef](#)] [[PubMed](#)]

2. Khan, M.A.; Jin, S.O.; Lee, S.H.; Chung, H.Y. Spectrofluorimetric determination of vitamin B₁ using horseradish peroxidase as catalyst in the presence of hydrogen peroxide. *Luminescence* **2009**, *24*, 73–78. [[CrossRef](#)] [[PubMed](#)]
3. Chen, Y.; Tian, F. Enzymatic Catalytic Spectrophotometric Determination of Thiamine in Food. *Food Anal. Method* **2009**, *3*, 7–11. [[CrossRef](#)]
4. Vignisse, J.; Sambon, M.; Gorlova, A.; Pavlov, D.; Caron, N.; Malgrange, B.; Shevtsova, E.; Svistunov, A.; Anthony, D.C.; Markova, N.; et al. Thiamine and benfotiamine prevent stress-induced suppression of hippocampal neurogenesis in mice exposed to predation without affecting brain thiamine diphosphate levels. *Mol. Cell Neurosci.* **2017**, *82*, 126–136. [[CrossRef](#)]
5. Stoffel, S.A.; Rodenko, B.; Schweingruber, A.M.; MäSer, P.; de Koning, H.P.; Schweingruber, M.E. Biosynthesis and uptake of thiamine (vitamin B₁) in bloodstream form *Trypanosoma brucei brucei* and interference of the vitamin with melarsen oxide activity. *Int. J. Parasitol.* **2006**, *36*, 229–236. [[CrossRef](#)]
6. Shankar, S.; John, S.A. Sensitive and highly selective determination of vitamin B₁ in the presence of other vitamin B complexes using functionalized gold nanoparticles as fluorophore. *RSC Adv.* **2015**, *5*, 49920–49925. [[CrossRef](#)]
7. Gong, F.; Zou, W.; Wang, Q.; Deng, R.; Cao, Z.; Gu, T. Polymer nanoparticles integrated with excited-state intramolecular proton transfer-fluorescent modules as sensors for the detection of vitamin B₁. *Microchem. J.* **2019**, *148*, 767–773. [[CrossRef](#)]
8. Gupta, R.K.; Yadav, S.K.; Saraswat, V.A.; Rangan, M.; Srivastava, A.; Yadav, A.; Trivedi, R.; Yachha, S.K.; Rathore, R.K. Thiamine deficiency related microstructural brain changes in acute and acute-on-chronic liver failure of non-alcoholic etiology. *Clin. Nutr.* **2012**, *31*, 422–428. [[CrossRef](#)] [[PubMed](#)]
9. Zera, K.; Zastre, J. Stabilization of the hypoxia-inducible transcription Factor-1 alpha (HIF-1 α) in thiamine deficiency is mediated by pyruvate accumulation. *Toxicol. Appl. Pharmacol.* **2018**, *355*, 180–188. [[CrossRef](#)]
10. Rocha, F.R.P.; Fatibello, O.; Reis, B.F. A multicommutated flow system for sequential spectrophotometric determination of hydrosoluble vitamins in pharmaceutical preparations. *Talanta* **2003**, *59*, 191–200. [[CrossRef](#)]
11. Rebwar, O.H.; Hunar, Y.M.; Hijran, S.J. Simultaneous spectrophotometric determination of thiamine and pyridoxine in multivitamin dosage forms using H-point standard addition and Vierordt's methods. *J. Iran. Chem. Soc.* **2018**, *15*, 1603–1612. [[CrossRef](#)]
12. Du, J.X.; Li, Y.H.; Lu, J.R. Flow injection chemiluminescence determination of thiamine based on its enhancing effect on the luminol-hydrogen peroxide system. *Talanta* **2002**, *57*, 661–665. [[CrossRef](#)]
13. Chen, J.; Li, B.Q.; Cui, Y.Q.; Yu, E.; Zhai, H.L. A fast and effective method of quantitative analysis of VB₁, VB₂ and VB₆ in B-vitamins complex tablets based on three-dimensional fluorescence spectra. *J. Food Compos. Anal.* **2015**, *41*, 122–128. [[CrossRef](#)]
14. Lynch, P.L.M.; Young, I.S. Determination of thiamine by high-performance liquid chromatography. *J. Chromatogr. A* **2000**, *881*, 267–284. [[CrossRef](#)]
15. Alizadeh, T.; Akhoundian, M.; Ganjali, M.R. An innovative method for synthesis of imprinted polymer nanomaterial holding thiamine (vitamin B₁) selective sites and its application for thiamine determination in food samples. *J. Chromatogr. B* **2018**, *1084*, 166–174. [[CrossRef](#)]
16. Perez-Ruiz, T.; Martinez-Lozano, C.; Sanz, A.; Guillen, A. Successive determination of thiamine and ascorbic acid in pharmaceuticals by flow injection analysis. *J. Pharmaceut. Biomed. Anal.* **2004**, *34*, 551–557. [[CrossRef](#)]
17. Luo, Y.W.; Miao, H.; Yang, X.M. Glutathione-stabilized Cu nanoclusters as fluorescent probes for sensing pH and vitamin B₁. *Talanta* **2015**, *144*, 488–495. [[CrossRef](#)]
18. Barrales, P.O.; Vidal, A.D.; de Cordova, M.L.F.; Diaz, A.M. Simultaneous determination of thiamine and pyridoxine in pharmaceuticals by using a single flow-through biparameter sensor. *J. Pharm. Biomed. Anal.* **2001**, *25*, 619–630. [[CrossRef](#)]
19. Akyilmaz, E.; Yasa, I.; Dinckaya, E. Whole cell immobilized amperometric biosensor based on *Saccharomyces cerevisiae* for selective determination of vitamin B₁ (thiamine). *Anal. Biochem.* **2006**, *354*, 78–84. [[CrossRef](#)]
20. Sinduja, B.; John, S.A. Highly selective naked eye detection of vitamin B₁ in the presence of other vitamins using graphene quantum dots capped gold nanoparticles. *New J. Chem.* **2019**, *43*, 2111–2117. [[CrossRef](#)]
21. Chen, Y.; Chen, T.; Wu, X.; Yang, G.J.S. Oxygen Vacancy-Engineered PEGylated MoO_{3-x} Nanoparticles with Superior Sulfite Oxidase Mimetic Activity for Vitamin B₁ Detection. *Small* **2019**, *15*, 46. [[CrossRef](#)]
22. Ge, J.; Lei, J.D.; Zare, R.N. Protein-inorganic hybrid nanoflowers. *Nat. Nanotechnol.* **2012**, *7*, 428–432. [[CrossRef](#)]
23. Huang, Y.Y.; Ran, X.; Lin, Y.H.; Ren, J.S.; Qu, X.G. Self-assembly of an organic-inorganic hybrid nanoflower as an efficient biomimetic catalyst for self-activated tandem reactions. *Chem. Commun.* **2015**, *51*, 4386–4389. [[CrossRef](#)]

24. Gao, J.; Liu, H.; Pang, L.; Guo, K.; Li, J. Biocatalyst and Colorimetric/Fluorescent Dual Biosensors of H₂O₂ Constructed via Hemoglobin-Cu₃(PO₄)₂ Organic/Inorganic Hybrid Nanoflowers. *ACS Appl. Mater. Inter.* **2018**, *10*, 30441–30450. [[CrossRef](#)]
25. Lin, Z.; Xiao, Y.; Yin, Y.Q.; Hu, W.L.; Liu, W.; Yang, H.H. Facile Synthesis of Enzyme-Inorganic Hybrid Nanoflowers and Its Application as a Colorimetric Platform for Visual Detection of Hydrogen Peroxide and Phenol. *ACS Appl. Mater. Inter.* **2014**, *6*, 10775–10782. [[CrossRef](#)]
26. Tian, R.; Zhang, B.Y.; Zhao, M.M.; Zou, H.J.; Zhang, C.H.; Qi, Y.F.; Ma, Q. Fluorometric enhancement of the detection of H₂O₂ using different organic substrates and a peroxidase-mimicking polyoxometalate. *RSC Adv.* **2019**, *9*, 12209–12217. [[CrossRef](#)]
27. Tian, R.; Zhang, B.Y.; Zhao, M.M.; Ma, Q.; Qi, Y.F. Polyoxometalates as promising enzyme mimics for the sensitive detection of hydrogen peroxide by fluorometric method. *Talanta* **2018**, *188*, 332–338. [[CrossRef](#)]
28. Zhang, B.Y.; Zhao, M.M.; Qi, Y.F.; Tian, R.; Carter, B.B.; Zou, H.J.; Zhang, C.H.; Wang, C.Y. The Intrinsic Enzyme Activities of the Classic Polyoxometalates. *Sci. Rep.* **2019**, *9*, 1. [[CrossRef](#)]
29. Sun, J.; Li, C.; Qi, Y.; Guo, S.; Liang, X.J.S. Optimizing Colorimetric Assay Based on V₂O₅ Nanozymes for Sensitive Detection of H₂O₂ and Glucose. *Sensors* **2016**, *16*, 584. [[CrossRef](#)]
30. Tian, R.; Sun, J.H.; Qi, Y.F.; Zhang, B.Y.; Guo, S.L.; Zhao, M.M. Influence of VO₂ Nanoparticle Morphology on the Colorimetric Assay of H₂O₂ and Glucose. *Nanomaterials* **2017**, *7*, 347. [[CrossRef](#)]
31. Krstonosic, V.; Milanovic, M.; Dokic, L. Application of different techniques in the determination of xanthan gum-SDS and xanthan gum-Tween 80 interaction. *Food Hydrocoll.* **2019**, *87*, 108–118. [[CrossRef](#)]
32. Kreuter, J. Influence of the Surface Properties on Nanoparticle-Mediated Transport of Drugs to the Brain. *J. Nanosci. Nanotechnol.* **2004**, *4*, 484–488. [[CrossRef](#)]
33. Garcia-Herrero, V.; Torrado-Salmeron, C.; Garcia-Rodriguez, J.J.; Torrado, G.; Torrado-Santiago, S. Submicellar liquid chromatography with fluorescence detection improves the analysis of naproxen in plasma and brain tissue. *J. Sep. Sci.* **2019**, *42*, 1702–1709. [[CrossRef](#)]
34. Zawaneh, A.H.; Khalil, N.N.; Ibrahim, S.A.; Al-Dafiri, W.N.; Maher, H.M. Micelle-enhanced direct spectrofluorimetric method for the determination of linifanib: Application to stability studies. *Luminescence* **2017**, *32*, 1162–1168. [[CrossRef](#)]
35. Abd El-Hay, S.S.; Belal, F.F. Development of a micelle-enhanced high-throughput fluorometric method for determination of niclosamide using a microplate reader. *Luminescence* **2019**, *34*, 48–54. [[CrossRef](#)]
36. Edwards, K.A.; Randall, E.A.; Tu-Maung, N.; Sannino, D.R.; Feder, S.; Angert, E.R.; Kraft, C.E. Periplasmic binding protein-based magnetic isolation and detection of thiamine in complex biological matrices. *Talanta* **2019**, *205*, 120168. [[CrossRef](#)]
37. Zhang, H.; Chen, H.Y.; Li, H.X.; Pan, S.; Ran, Y.L.; Hu, X.L. Construction of a novel turn-on-off fluorescence sensor used for highly selective detection of thiamine via its quenching effect on o-phen-Zn²⁺ complex. *Luminescence* **2018**, *33*, 1128–1135. [[CrossRef](#)]
38. Tan, H.L.; Li, Q.; Zhou, Z.C.; Ma, C.J.; Song, Y.H.; Xu, F.G.; Wang, L. A sensitive fluorescent assay for thiamine based on metal-organic frameworks with intrinsic peroxidase-like activity. *Anal. Chim. Acta* **2015**, *856*, 90–95. [[CrossRef](#)]
39. Purbia, R.; Paria, S. A simple turn on fluorescent sensor for the selective detection of thiamine using coconut water derived luminescent carbon dots. *Biosens. Bioelectron.* **2016**, *79*, 467–475. [[CrossRef](#)]
40. Perez-Ruiz, T.; Martinez-Lozano, C.; Tomas, V.; Ibarra, I.J.T. Flow injection fluorimetric determination of thiamine and copper based on the formation of thiochrome. *Talanta* **1992**, *39*, 907. [[CrossRef](#)]

Publisher's Note: MDPI stays neutral with regard to jurisdictional claims in published maps and institutional affiliations.



© 2020 by the authors. Licensee MDPI, Basel, Switzerland. This article is an open access article distributed under the terms and conditions of the Creative Commons Attribution (CC BY) license (<http://creativecommons.org/licenses/by/4.0/>).